Evidence for Landau's critical velocity in superfluid helium nanodroplets from wave packet dynamics of attached potassium dimers

Martin Schlesinger[1],[*] Marcel Mudrich[2], Frank Stienkemeier[2], and Walter T. Strunz[1]

[1]*Institut für Theoretische Physik, Technische Universität Dresden, D-01062 Dresden, Germany and*
[2]*Physikalisches Institut, Universität Freiburg, D-79104 Freiburg, Germany*

Femtosecond pump-probe spectroscopy has been used to study vibrational dynamics of potassium dimers attached to superfluid helium nanodroplets. Comparing the measured data with theoretical results based on dissipative quantum dynamics we propose that the most important effect of the helium environment is a general damping of the vibrational dynamics as a result of the interaction between dimer and collective degrees of freedom of the helium droplet. The calculations allow us to explain crucial experimental findings that are unobserved in gas-phase measurements. Remarkably, best agreement with experiment is found for a model where we neglect damping once a wave packet moves below a critical velocity. In this way the results provide first direct evidence for the Landau critical velocity in superfluid nanodroplets.

Superfluidity in finite-sized quantum systems is a fundamental issue of current interest, both in liquid helium (He) [1, 2, 3] and in ultracold atomic gases [4]. As first discussed by Landau, superfluidity manifests itself through the fascinating effect of frictionless flow below a critical velocity [5]. In this Letter we present direct evidence for the existence of a critical velocity in superfluid He nanodroplets.

Spectroscopy of probe molecules embedded inside He clusters and He nanodroplets ($10^3 - 10^4$ atoms) has provided some insight into their superfluid behaviour by studying the response to external perturbations [1, 2, 3]. In contrast to pure spectroscopic studies reported earlier, we present femtosecond pump-probe measurements. This technique is well-established for studying vibrational wave packet (WP) dynamics of diatomic systems [6, 7, 8, 9, 10]. Here, we investigate potassium molecules (K_2) attached to He nanodroplets (He nanodroplet isolation (HENDI) spectroscopy) [11]. He droplets provide a versatile test bed for studying relaxation dynamics of the immersed species which are cooled to the droplet temperature (0.38 K) [12, 13].

The observed real time pump-probe spectra of K_2 on He droplets differ significantly from previously obtained gas phase results [11, 14]. In this paper we argue that dissipative quantum dynamics, here employed through a quantum master equation, is crucial for the understanding of these measurements. Moreover, the dissipation has to be combined with stochastic desorption of the molecule and shifts of the potential energy surfaces induced by the He droplets to correctly describe the experimental results. Remarkably, we find best agreement with the experimental findings when damping is omitted for very slowly moving WPs. This demonstrates the potential of real time studies of vibrational motions to investigate the Landau critical velocity on the microscopic scale, very much in the spirit of vibrational wire resonators [15] or quartz tuning forks [16] that probe on larger scales.

In the pump-probe spectroscopy of K_2, potassium atoms are attached to He nanodroplets ($\sim 5\,000$ atoms) which are created in a supersonic expansion of He gas at cryogenic conditions [11]. Doping conditions are chosen such that on average two potassium atoms stick to one droplet forming K_2 dimers which are weakly bound on the surface of the droplets. In a one color pump-probe excitation scheme the resulting K_2^+ photo ions are recorded mass selectively. A laser having 110 fs pulse width has been used providing 16 nJ pulses mildly focused in the interaction region with the molecular beam. The (3)-photon excitation schemes which are most relevant are depicted in Fig. 1.

The time dependent Schrödinger equation for the state $\Psi(t) = (\psi_X(t), \psi_A(t), \dots)$ is solved fully numerically, as detailed for the gas phase in Refs. [8, 17]. Here, $\psi_i(t)$ denotes the vibrational WP in electronic state i. Transition dipole moments are assumed to be constant (Condon approximation). In a first step we include He-induced shifts of potential energy surfaces (PES). Systematic numerical tests reveal that best agreement with experiment is obtained when only shifting the 2Π surface (by -50cm^{-1}) which agrees well with findings in [11, 18]. As the excess energy of photo electrons is not observed here, a shift of the ionic surface as reported in [19] has no effect on our results. Next, we take into account dimer desorption from the droplets. We choose a constant desorption rate leading to a probability density $P(t') \sim \exp\{-t'/\tau_D\}$ for the desorption time t' after electronic excitation. Upon desorption, the He-induced shifts are set to zero. We find that a description solely based on energy shift (parameter Δ_Π) and desorption (parameter τ_D) cannot reproduce crucial features of the HENDI measurements [20].

The new essential ingredient of our description is the inclusion of damping of vibrational WPs. Dissipation of vibrational energy occurs due to the interaction with
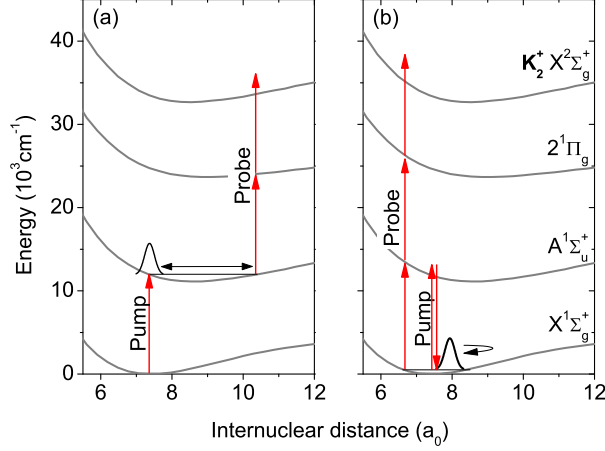
FIG. 1: Potential curves of the K_2 molecule and excitation schemes at $\lambda = 833$ nm (a) and at $\lambda = 800$ nm (b). The pump pulse creates vibrational WPs in various electronic states. Significant ionization through the probe pulse occurs in (a) only if a WP is located around the outer, and in (b) only if a wave packet is near the inner turning point (FC window).

collective degrees of freedom of the He droplets (phonons or ripplons). In our phenomenological approach we do not specify the microscopic dimer-droplet interaction. Instead, we use a well-established master equation, describing damping for near-harmonic systems at effectively zero temperature fully quantum mechanically (see [22]). Thus, the dynamics of the full vibrational density operator ρ is determined from

$$\dot{\rho} = -\frac{i}{\hbar}[H, \rho] + \frac{1}{2}\sum_i \gamma_i \left(2a_i\rho a_i^\dagger - a_i^\dagger a_i \rho - \rho a_i^\dagger a_i\right). \quad (1)$$

Here, H denotes the vibrational Hamiltonian and $a_i, a_i^\dagger$ are the annihilation/creation operators obtained from a harmonic approximation of the PES corresponding to electronic state i. We choose the parameters for damping (rates $\gamma_i \equiv \gamma$) and desorption (time τ_D) to be state-independent. Note, however, a possible influence of the orientation of the dimer on damping dynamics as discussed for Li_2 in [21]. We here assume no change of alignment during dynamics.

Excitation at a wavelength of 833 nm almost exclusively follows the path sketched in Fig. 1 (a) and probes the WP propagation in the $A^1\Sigma_u^+$ electronic state [10]. The probe pulse leads to an enhanced population of the final ionic state only if the WP is located at the outer turning point, where the intermediate 2Π state opens a Franck-Condon (FC) window. The resulting oscillatory structure (Fig. 2) in the ion rate reflects the dynamics of the WP in the A state. The simulation of the ion signal for the gas phase is shown in Fig. 2(b) and agrees

with earlier gas phase results [8]. The weak overall decrease of the oscillation amplitude in Fig. 2(b) is caused by the spreading of the initially well-localized WP in the anharmonic potential. This gas phase result is markedly different from the experimental HENDI spectrum (Fig. 2 (a)), which is a clear sign of the effect of the He environment. The measured signal shows an exponential decay of the initial amplitude which is well captured by our calculations (Fig. 2 (c)). The persisting oscillations are also reproduced, yet with a smaller amplitude.

Best agreement between experiment and our theory is obtained when damping, shift and desorption are included into the calculation with parameters $\gamma = 0.15/\text{ps}$, $\Delta_\Pi = -50$ cm^{-1} and $\tau_D = 8$ ps (Fig. 2 (c)). The dependence of all our findings on these precise values is rather smooth and only after leaving a $\pm 5\%$ interval significant deviations from the displayed figures occur.

It is tempting to relate the damping rate γ to measurements of the viscosity η in liquid He (see [16]). However, such values for η are based on macroscopic theories which are not applicable here. Note that in [21] the authors investigate dissipative alkali dimer dynamics on a microscopic scale by studying collisions with ^{4}He atoms. Remarkably, the calculated friction coefficient for singlet systems (0.06/ps) turns out to be of the order of magnitude of our γ.

The temporal evolution and intensity of certain frequency components can be visualized by employing sliding window Fourier transforms (FT) on the time-dependent signal ("spectrogram" [9]). As discussed in Ref. [11], in the experiment at 833 nm excitation wave
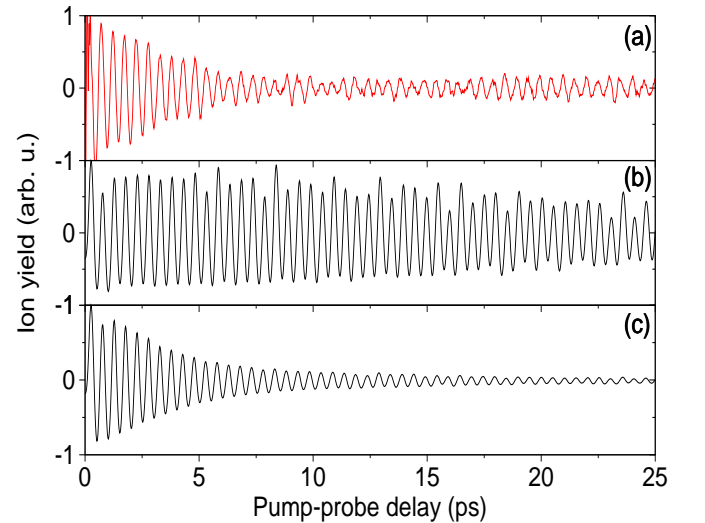

FIG. 2: Pump-probe signal for $\lambda = 833$ nm. (a) Experimental HENDI result (from Ref. [11]); (b) Numerical simulation for the gas phase (see also [8]); (c) Calculated signal assuming He-induced damping, shift of PES and desorption of the molecule.

length a small increase of the frequency of the WP motion during the first 10 ps is observed. In Fig. 3 this behavior (if less pronounced) is seen in the FT spectrum of our calculated signal, provided damping is included. The findings allow the following interpretation: during the first few picoseconds the contribution of the damped molecules is most important. As a consequence of the anharmonic potential, they vibrate with a higher frequency, explaining the initial shift of the main frequency ω_A^{833nm} to slightly larger values (or lower vibrational quantum numbers). Later on, for times $\tau > 10$ ps, vibrationally damped molecules no longer contribute, as a closing of their FC window takes place. Hence, only molecules which desorb very early and thus do not suffer vibrational damping contribute to the ion yield at late delay times. Consequently, a weak oscillatory signal persists in the time domain and in the windowed FT the main frequency returns to the original gas phase value.

At the shorter wave length $\lambda = 800$ nm the excitation scheme sketched in Fig. 1 (b) applies. Here, a WP in the ground state, excited through stimulated Raman scattering (RISRS), can be visualized through 3-photon absorption. In the gas phase, this process is superposed coherently with transitions from higher lying electronic states near their respective inner turning points, leading to interferences in the ionic state. A more detailed analysis shows that in the gas phase the interference is indeed destructive: the contribution of the WP on the X surface is missing in the gas phase (see Fig. 4 (b)) – see similar findings in [23]. Without any damping mechanism, contributions from the A state (component $\omega_A^{800nm} \approx 64 cm^{-1}$) and from the 2Π state (component $2\omega_{2\Pi}^{800nm} \approx 86 cm^{-1}$) are dominant, which is not observed in the He droplet experiment (Fig. 4(a)). There, although ω_A^{800nm} is present during the first 5 ps, it fades out and only the component $\omega_X^{800nm} \approx 91$ cm^{-1} (WP in X state) contributes at later delay times. We now include damping for $\lambda = 800$ nm with precisely the same parameters as for the considerations at $\lambda = 833$ nm. The correspond-

FIG. 4: Spectrograms showing the WP dynamics at $\lambda = 800$ nm for the experimental HENDI result (a), for the gas-phase simulation (b), for the fully damped model (c), and for simulated data including a critical velocity (d).
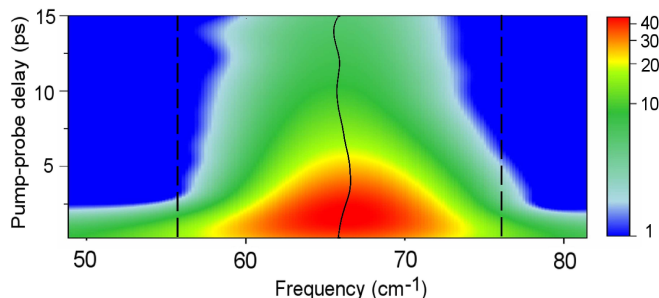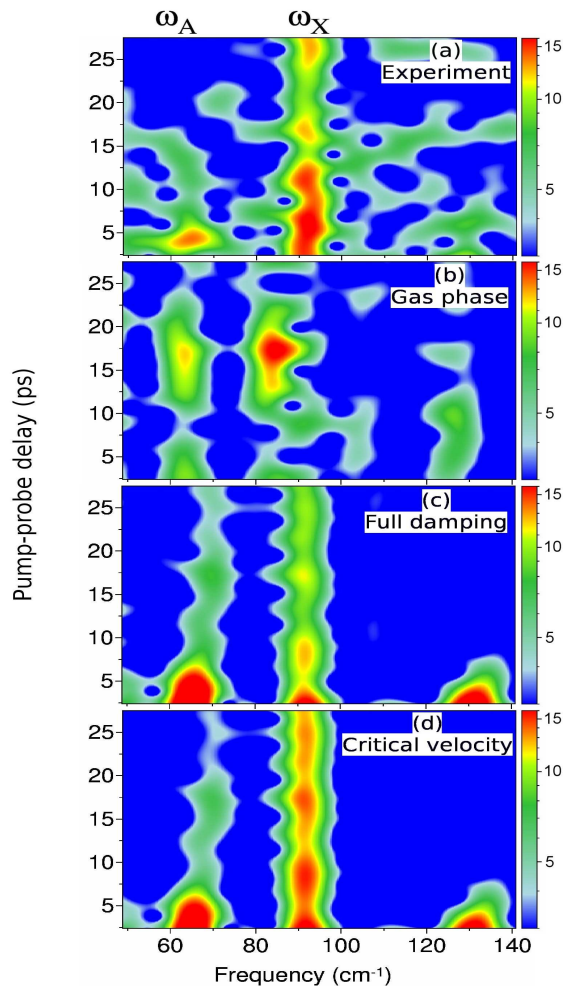

FIG. 3: Calculated pump-probe signal for $\lambda = 833$ nm. The dominant frequency is slightly shifted to larger values for short delay times (the black solid line indicates the the mean frequency between the dashed lines as a function of time).

ing spectrogram (Fig. 4(c)) agrees remarkably well with experimental findings in many respects. The component at ω_A^{800nm} fades out after several ps due to vibrational damping: the WP in the A state leaves the initial FC window at the inner turning point.

More significant is the behavior of the component near ω_X^{800nm}, ascribed to the ground state WP. It is clearly visible in the experimental and theoretical (including damping) spectrogram, yet absent in the gas phase. Damping of the WPs in the A and 2Π state enhances ionization from the ground state by the probe pulse, since the mapping of the X state dynamics to the ion no longer suffers from destructive interference with competing processes near the inner turning point on the A and 2Π surfaces. Most remarkably, the results at 800 nm hint at a direct influence of superfluidity on these spectra. Molecules are assumed to be able to move unhindered through a superfluid as long as their velocity does not exceed the
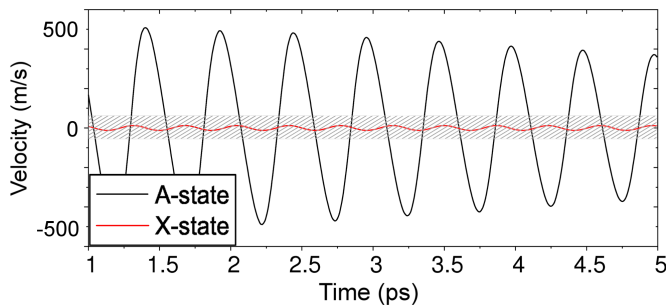
FIG. 5: Dynamics in velocity domain of a WP excited in the electronically excited A-state and in the ground state X. The hatched area indicates velocities below the critical value of 60 m/s.

(Landau) critical velocity v_c [5]. In a simple approach we determine from our calculations the average velocity $\langle v \rangle = \langle \hat{P} \rangle / 2\mu$ of the nuclear WP. Once it drops below the critical velocity (we chose the bulk value $v_c = 60$ m/s), we set the friction coefficient to zero (see also [24]) and compare with the fully damped model.

Fig. 5 illustrates the WP velocities in the ground (X) and excited state (A). For the excitation at $\lambda = 833$ nm, it is the dynamics on the A surface that dominates the observations. This vibration, however, is fast and the corresponding velocity oscillates between ± 500 m/s. For most of the time, therefore, friction is present and the influence of v_c is hardly noticeable. For an excitation at wave length $\lambda = 800$ nm, however, the motion on the X surface is so slow (at most $v \approx 15$ m/s) that we neglect damping on that surface entirely ($\gamma_X = 0$). In the resulting spectrogram (Fig. 4(d)), the component $\omega_X^{800\mathrm{nm}}$ is even more pronounced compared to the previous calculation (full damping). Most strikingly, the agreement with the experimental result is improved.

In conclusion, the study of vibrational wave packets in dimers attached to He nanodroplets exhibits clear deviations from previous gas phase results. A model based on shifts of potential energy surfaces, desorption from the host and, most importantly, damping of the wave packets is able to explain crucial features of the measurement. For excitation at $\lambda = 833$ nm the decay of the signal and a small shift in the FT spectrum are reproduced. Damping of excited state wave packets enhances the mapping of the ground state dynamics to the ion signal, as realized at $\lambda = 800$ nm.

Most remarkably, in our studies best agreement with experiment is obtained when we neglect damping for very slowly moving wave packets. We attribute this observation to the role of the critical velocity in these experiments, which turns out to be larger than the velocity of the motion on the X surface. Thus, the influence of superfluidity is directly visible, opening the door for further studies: choosing heavier molecules for which the vibra-

tional velocities are well below some 100 m/s, in combination with a microscopic fully quantum calculation will enable us to investigate friction and frictionless motion on the atomic scale.

---

[*] Electronic address: Martin.Schlesinger@tu-dresden.de
[1] M. Hartmann, F. Mielke, J. P. Toennies, A. F. Vilesov, and G. Benedek, Phys. Rev. Lett. **76**, 4560 (1996).
[2] S. Grebenev, J. P. Toennies, and A. F. Vilesov, Science **279**, 2083 (1998).
[3] J. Tang, Y. J. Xu, A. R. W. McKellar, and W. Jäger, Sience **297**, 2030 (2002).
[4] J. R. Anglin and W. Ketterle, Nature **416**, 211 (2002).
[5] L. Landau, Journal Of Physics-USSR **5**, 71 (1941).
[6] R. Bowman, M. Dantus, and A. Zewail, Chem. Phys. Lett. **161**, 297 (1989).
[7] T. Baumert, V. Engel, C. Röttgermann, W. T. Strunz, and G. Gerber, Chem. Phys. Lett. **191**, 639 (1992).
[8] R. de Vivie-Riedle, K. Kobe, J. Manz, W. Meyer, B. Reischl, S. Rutz, E. Schreiber, and L. Wöste, J. Phys. Chem. **100**, 7789 (1996).
[9] S. Rutz and E. Schreiber, Chem. Phys. Lett. **269**, 9 (1997).
[10] C. Nicole, M. A. Bouchène, C. Meier, S. Magnier, E. Schreiber, and B. Girard, J. Chem. Phys. **111**, 7857 (1999).
[11] P. Claas, G. Droppelmann, C. P. Schulz, M. Mudrich, and F. Stienkemeier, J. Phys. B **39**, S1151 (2006).
[12] J. P. Toennies and A. F. Vilesov, Angewandte Chemie **43**, 2622 (2004).
[13] F. Stienkemeier and K. K. Lehmann, J. Phys. B: At. Mol. Opt. Phys. **39**, R127 (2006).
[14] K. Nauta and R. E. Miller, J. Chem. Phys. **113**, 9466 (2000).
[15] A. Kraus, A. Erbe, and R. H. Blick, Nanotechnology **11**, 165 (2000); C. A. M. Castelijns, K. F. Coates, A. M. Guenault, S. G. Mussett, and G. R. Pickett, Phys. Rev. Lett. **56**, 69 (1986).
[16] A. A. Zadorozhko, E. Y. Rudavskii, V. K. Chagovets, and G. A. Sheshin, Low Temp. Phys. **35**, 100 (2009).
[17] R. de Vivie-Riedle, B. Reischl, S. Rutz, and E. Schreiber, J. Phys. Chem. **99**, 16829 (1995).
[18] P. Claas, Ph.D. thesis, Universität Bielefeld (2006).
[19] E. Loginov, D. Rossi, M. Drabbels, Phys. Rev. Lett. **95**, 163401 (2005).
[20] M. Schlesinger and W. T. Strunz, *in preparation* (2009).
[21] S. Bovino, E. Coccia, E. Bodo, E. Lopez-Duran, and F. A. Gianturco, J. Chem. Phys. **130**, 224903 (2009)
[22] M. O. Scully and M. S. Zubairy, *Quantum Optics* (Cambridge University Press, 1997).
[23] T. Baumert, V. Engel, C. Meyer, and G. Gerber, Chem. Phys. Lett. 200; 488 (1992).

[24] D. Bonhommeau, A. Viel, and N. Halberstadt, J. Chem. Phys. **120**, 11359 (2004).